ACS APPLIED MATERIALS & INTERFACES

Research Article

www.acsami.org

DRIFT Study of $CuO-CeO_2-TiO_2$ Mixed Oxides for NO_x Reduction with NH_3 at Low Temperatures

Lei Chen,[†] Zhichun Si,[†] Xiaodong Wu,[†,‡] and Duan Weng*[,†,‡]

[†]Graduate School at Shenzhen, Tsinghua University, Shenzhen 518055, China

[‡]State Key Lab of New Ceramics and Fine Processing, School of Materials Science and Engineering, Tsinghua University, Beijing 100084, China

ABSTRACT: A $CuO-CeO_2-TiO_2$ catalyst for selective catalytic reduction of NO_x with NH_3 (NH_3-SCR) at low temperatures was prepared by a sol–gel method and characterized by X-ray diffraction, Brunner–Emmett–Teller surface area, ultraviolet–visible spectroscopy, H_2 temperature-programmed reduction, scanning electron microscopy and in situ diffuse reflectance infrared Fourier transform spectroscopy (in situ DRIFTS). The $CuO-CeO_2-TiO_2$ ternary oxide catalyst shows excellent NH_3-SCR activity in a low-temperature range of 150–250 °C. Lewis acid sites generated from Cu^{2+} are the main active sites for ammonia activation at low temperature, which is crucial for low temperature NH_3-SCR activity. The introduction of ceria results in increased reducibility of CuO species and strong interactions between CuO particles with the matrix. The interactions between copper, cerium and titanium oxides lead to high dispersion of metal oxides with increased active oxygen and enhanced catalyst acidity. Homogeneously mixed metal oxides facilitate the "fast SCR" reaction among Cu^{2+}–NO, nitrate (coordinated on cerium sites) and ammonia (on titanium sites) on the $CuO-CeO_2-TiO_2$ catalyst at low temperatures.

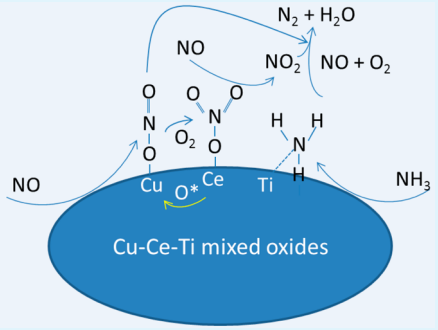

KEYWORDS: *NH_3-SCR, $CuO-CeO_2-TiO_2$, acid sites, strong interactions, DRIFTS*

1. INTRODUCTION

Nitrogen oxides (NO_x) are the major air pollutant contributors to acid rain, photochemical smog and ozone depletion.[1−4] Chinese legislation of NO_x emissions from both stationary and mobile sources is increasingly stringent.[2] NO_x removal at low temperatures is important for flue gas treatment, especially in cement and steel manufacturing. Selective catalytic reduction of NO_x with (NH_3-SCR) is a typical commercial technique for the abatement of NO_x, in which $V_2O_5-WO_3(MoO_3)-TiO_2$ is the most commonly used catalyst. However, vanadium catalyst limitations, including vanadium toxicity and poor activity in the low temperature range, constrain their usage in low-temperature applications. Developing low-temperature NH_3-SCR catalysts is still a challenge, especially for applications below 200 °C.[2]

The standard NH_3-SCR reaction stoichiometry is shown in eq 1. At low temperatures, the reaction between NH_3 and NO_x (equimolar of NO and NO_2) in feed gas is much faster than the standard NH_3-SCR reaction and thus termed the "fast SCR" reaction (eq 2).[5−11] A catalyst that can take advantage of this fast SCR would possess the low-temperature deNO_x.

$$4NH_3 + 4NO + O_2 \rightarrow 4N_2 + 6H_2O \quad (1)$$

$$2NH_3 + NO + NO_2 \rightarrow 2N_2 + 3H_2O \quad (2)$$

Several transitional metal oxides, including MnO_x, CeO_2, CuO_x, NiO, FeO_x and inclusive mixed oxides, have been reported as active for low-temperature NH_3-SCR reactions and attracted great attention in recent years.[2,4,12−15] MnO_x and other manganese-containing catalysts present promising NO_x conversions in the range of 100–200 °C. However, improvement in N_2 selectivity and poisoning resistance to H_2O and sulfur oxides at low temperatures is important for low-temperature applications.[2] Alternatively, copper-containing catalysts, mostly in the form of Cu exchanged zeolites such as Cu/SAPO-34, also show superior low-temperature activity. Due to the high cost of copper exchanged zeolites, copper-containing mixed oxide catalysts have also been developed. In our previous work,[15] CuO_x impregnated on the coprecipitated WO_3-ZrO_2 support shows high SCR activity in the range 200–320 °C. The acidity of the WO_3-ZrO_2 support allows improved ammonia adsorption, essential for high SCR activity. Sullivan et al.[16] reported that copper oxide based catalysts prepared from two different precursors ($Cu(NO_3)_2$ and $CuSO_4$) with various oxide supports (SiO_2, TiO_2 and Al_2O_3) are also active in the NH_3-SCR reaction. Other copper based catalysts, such as CuMoCe[17] and CuMnTi,[18] also show remarkable NH_3-SCR activities between 200 and 300 °C.

Ceria is well-known for its excellent oxygen storage capacity and high redox ability via Ce^{4+} to Ce^{3+} transition.[19−21] Ceria can also act as an active component in the SCR reaction and has thus been extensively studied for this application.

Received: January 23, 2014
Accepted: May 21, 2014
Published: May 21, 2014

 © 2014 American Chemical Society dx.doi.org/10.1021/am5004969 | *ACS Appl. Mater. Interfaces* 2014, 6, 8134–8145

Specifically, CeO_2-TiO_2 catalysts have been reported to possess high activity, excellent N_2 selectivity and high tolerance to SO_2 and H_2O in the NH_3-SCR reaction.[22−24] The cheap and easy combination of copper oxide and ceria provides novel catalysts with excellent low-temperature activity and sulfur/H_2O resistance. Gao Xiang et al.[25−27] reported that a CeTi catalyst, modified by introduction of a low copper concentration (3.7 wt %), presented high SCR activity at low temperatures due to the formation of active oxygen species from the strong interaction between Ce and Cu. This CeCuTi catalyst also showed high SO_2 resistance, which was ascribed to the sacrificial formation of $CuSO_4$, preserving Ce^{4+} active sites.[26] However, CeCuTi catalysts with high copper oxide concentrations have not been systematically studied and associated NH_3-SCR reaction routes are still unclear.

In this study, a CuCeTi catalyst containing a high loading concentration of copper (preoptimized to 30 wt %) was exploited for a low-temperature NH_3-SCR catalyst. In situ diffuse reflectance infrared Fourier transform spectroscopy (in situ DRIFTS) was used to mechanistically elucidate the NH_3-SCR reaction pathway. The effect of strong interactions between copper, cerium and titanium on the NH_3-SCR reaction is also discussed.

2. EXPERIMENTAL SECTION

2.1. Catalyst Preparation. The CuCeTi mixed oxide catalysts were prepared by a step sol−gel method. Cupric nitrate (AR, Beijing Chem. Plant), cerium nitrate hexahydrate (AR, Aladdin), citric acid (AR, Aladdin), nitric acid (AR, Beijing Chem. Plant) and tetrabutyl titanate (AR, Beijing Chem. Plant) were used as precursors. Tetrabutyl titanate was added dropwise into 50 mL of an aqueous solution of nitric acid and citric acid to get the clear titanium solution, and then cupric nitrate and cerium nitrate hexahydrate were added into the titanium solution. The molar ratio of Cu:Ce:Ti was 3:1:6 and the molar ratio of metal components (Cu, Ce and Ti) to citric acid to nitric acid was 1:1.5:1.5. The solution was stirred and heated at 80 °C for 5 h to form a gel. Then the gel was dried at 110 °C for 12 h and calcined in a maffle furnace at 500 °C for 5 h. Finally, the samples were crushed and sieved to 50−80 mesh for catalytic activity measurements.

2.2. Catalyst Characterization. The powder X-ray diffraction (XRD) experiments were performed on a German Bruker D8 ADVANCE diffractometer employing Cu Kα radiation (λ = 0.154 18 nm). The X-ray tube was operated at 40 kV and 40 mA. The X-ray powder diffractogram was recorded at 6°/min in the range of 20° < 2θ < 80°. The identification of the phases was made with the help of JCPDS cards (Joint Committee on Powder Diffraction Standards).

The specific surface areas of the samples were measured using the N_2 physisorption at −196 °C by the Brunner−Emmett−Teller (BET) method using an automatic surface analyzer (F-sorb 3400, China). The samples were degassed in flowing N_2 at 200 °C for 2 h. The particle size of catalysts was measured by a Malvern Mastersizer 2000 particle size analyzer. The catalysts were centrifuged 3 min before each test. Volume average particle size was used to represent the average particle size of the samples.

The ultraviolet−visible (UV−vis) diffuse reflectance spectra were recorded over the wavelength range λ = 200−800 nm on a SHIMADZU UV-2450 spectrophotometer with integration sphere diffuse reflectance attachment. Samples were diluted by $BaSO_4$.

H_2 temperature-programmed reduction (H_2-TPR) experiments were conducted on a Micromeritics Autochem II 2920 chemisorption analyzer using 50 mg of the CuCeTi samples. The samples were preheated at 500 °C for 30 min in He flow. The temperature was increased from 50 to 1000 °C at a heating rate of 10 °C min^{-1} with 10% H_2/Ar gases. The H_2 consumption was recorded continuously.

Scanning electron micrographs along with elemental mappings using energy dispersive spectroscopy (EDS) of the catalysts were taken using scanning electron microscopy (LEO1530, Germany).

A thermo Nicolet 6700 Fourier transform infrared spectrometer was equipped with a high-temperature environmental cell fitted with a KBr window. In situ DRIFTS spectra of adsorbed species were recorded in the range of 4000−650 cm^{-1}. Prior to the adsorption, the sample was placed in a crucible located in a high-temperature cell and heated up to 500 °C in a 20% (v/v) O_2/N_2 flow mixture with a total flow of 100 mL for 30 min to remove traces of organic residues. After that, the sample was cooled down to the corresponding temperature and was flushed by 100 mL min^{-1} N_2 for 30 min to remove the physisorbed molecules for background collection. For the NH_3 adsorption, a gas mixture containing 1000 ppm of NH_3 in N_2 with a total flow rate of 100 mL min^{-1} passed through the sample for 60 min. After purging the weakly adsorbed or gaseous NH_3/NO_x molecules by N_2 flow for 30 min, the DRIFT spectra of adsorbed species on catalysts were collected simultaneously. The $NO+O_2$ adsorption and NH_3+NO+O_2 coadsorption similar procedures were carried out in a gas mixture containing 1000 ppm of NO + 5% O_2 in N_2 and 1000 ppm of NH_3 + 1000 ppm of NO + 5% O_2 in N_2, respectively.

For the $NO+O_2$ adsorption over the NH_3 preadsorbed catalysts, a similar procedure was carried out for the pretreatment and the background collection. The catalysts were preadsorbed with NH_3 for 30 min followed by 30 min of N_2 purging at 150 °C. The $NO+O_2$ was then introduced into the IR cell, and the spectra were recorded as a function of time. A similar procedure was carried out for the NH_3 adsorption over the $NO+O_2$ preadsorbed catalysts.

2.3. Activity Measurements. The catalytic activity measurement for the reduction of NO by ammonia (NH_3-SCR) with excess oxygen was carried out in a fixed bed reactor made of a quartz glass tube. 0.2 g of catalysts with 50−80 mesh was diluted to 1 mL by silica. The reactant gas mixture consisted of 500 ppm of NO, 500 ppm of NH_3, 5% O_2 and N_2 in balance. The activity of the catalyst was tested at various temperatures from 100 to 350 °C under stable a reaction atmosphere. The total flow of the gas mixture was 1 L min^{-1} at a gas hourly space velocity (GHSV) of 30 000 h^{-1}. The concentrations of nitrogen oxides and ammonia were measured at 120 °C by a Thermo Nicolet 380 DRIFT spectrometer equipped with 2 m path-length sample cell (250 mL volume). The gas path from the reactor to DRIFT spectrometer was maintained at a constant temperature of 120 °C to avoid NH_4NO_2/NH_4NO_3 deposition. The NO_x conversions were calculated as eq 3.

$$NO_x \text{ conversion } (\%) = 1 - \frac{NO_{out} + NI_{2out}}{NO_{in}} \times 100 \quad (3)$$

Ammonia oxidation and NO oxidation tests were carried out using a similar method to NH_3-SCR activity with 500 ppm of NH_3 (500 ppm of NO for NO oxidation) and 5% O_2 in N_2 balance.

3. RESULTS

3.1. Catalytic Activity for NH_3-SCR and NH_3/NO Oxidation. The NH_3-SCR activities of the catalysts are shown in Figure 1. The results indicate that the CuCeTi catalyst is most active in the temperature range of 150−250 °C. The CuTi catalyst shows lower activity within this temperature region, while the catalytic activity of the copper-containing catalyst decreases rapidly above 250 °C, which is mainly due to the low adsorption and over oxidation of NH_3 as the temperature increases. Alternatively, the CeTi catalyst only shows significant NO_x conversions above 250 °C. These results imply that copper oxides act as the main active site in low-temperature SCR reactions while cerium also plays an important role in improving catalytic activity.

N_2O is the major byproduct arising from copper-containing catalysts. As shown in Figure 1, N_2O formation occurs in SCR reactions at 150 °C and increases with reaction temperatures up to 350 °C. Remarkably, N_2O (60 ppm) is detected when the temperature up to 350 °C. These results indicate that the

dx.doi.org/10.1021/am5004969 | ACS Appl. Mater. Interfaces 2014, 6, 8134−8145

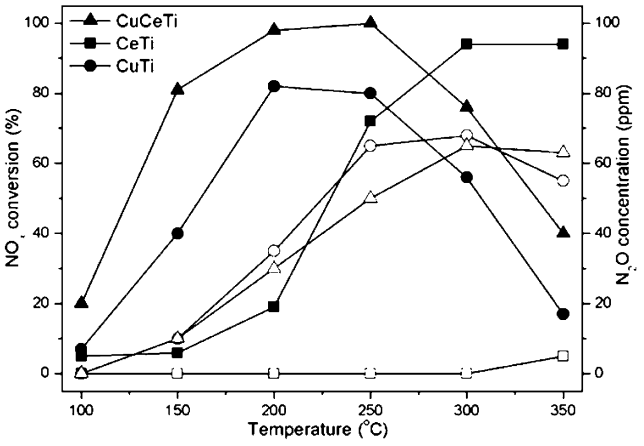

Figure 1. NH_3-SCR activities and N_2O formation of the catalysts as a function of temperature. Filled symbols, NO_x conversion; open symbols, N_2O concentration. Reaction conditions: [NO] = [NH_3] = 500 ppm, [O_2] = 5%, balanced in N_2, GHSV = 30 000 h^{-1}.

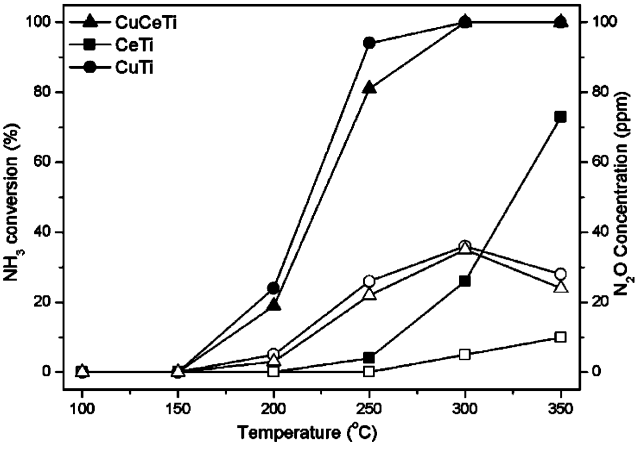

Figure 2. NH_3 oxidation activity and N_2O formation of the catalysts as a function of temperature. Filled symbols, NH_3 oxidation activity; open symbols, N_2O concentration. Reaction conditions: [NH_3] = 500 ppm, [O_2] = 5%, balanced in N_2, GHSV = 30 000 h^{-1}.

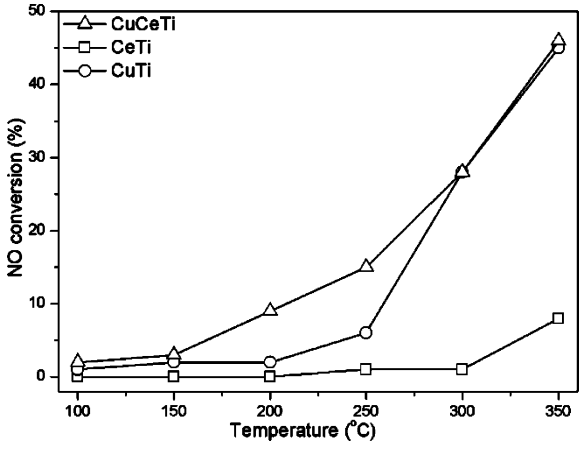

Figure 3. NO oxidation activities of the catalysts as a function of temperature. Reaction conditions: [NO] = 500 ppm, [O_2] = 5%, balanced in N_2, GHSV = 30 000 h^{-1}.

introduction of copper remarkably enhances NH_3-SCR activity at low temperatures with significantly increased N_2O selectivity.

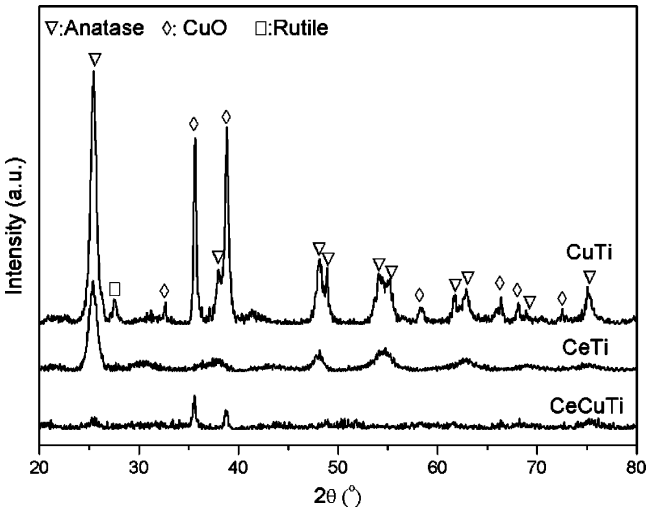

Figure 4. XRD patterns of the catalysts.

Table 1. Composition, BET Surface Areas and Particle Size of the Catalysts

	composition (mol %)				
catalysts	CeO_2	CuO	TiO_2	S_{BET} (m^2 g^{-1})	average particle size (um)
CeTi	10		90	59.1	38
CuTi		30	70	38.1	42
CuCeTi	10	30	60	77.8	33

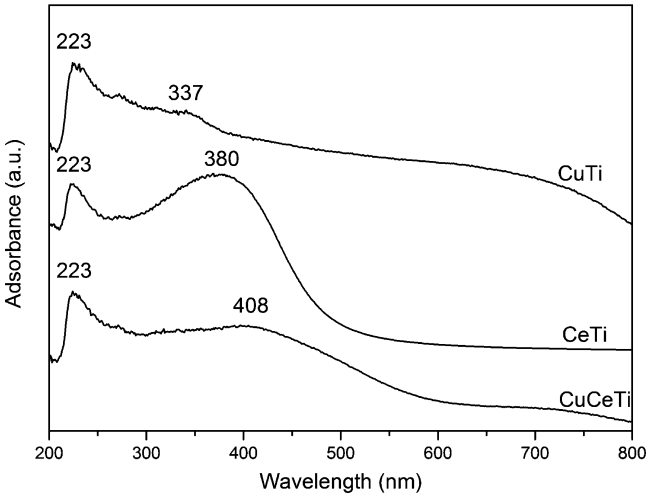

Figure 5. UV−vis spectra of CuCeTi catalysts.

Catalytic NH_3 oxidation activity and N_2O formation are shown in Figure 2. The copper-containing catalysts show similar NH_3 oxidation activities, which are much higher than that of CeTi. The NH_3 oxidation occurs at around 160 °C on copper-containing catalysts and at 240 °C on the CeTi catalyst. These results are in agreement with the fact that copper-containing catalysts are active in the oxidation of NH_3 as reported previously.[28] N_2O is detected and becomes the dominant product above 200 °C. Again, no distinct N_2O formation is detected from NH_3 oxidation on the CeTi catalyst. A comparison of Figures 1 and 2 indicates that increasing N_2O formation with increasing NH_3 oxidation is similar to that in NH_3-SCR reactions. However, the amount of N_2O generated in

dx.doi.org/10.1021/am5004969 | ACS Appl. Mater. Interfaces 2014, 6, 8134−8145

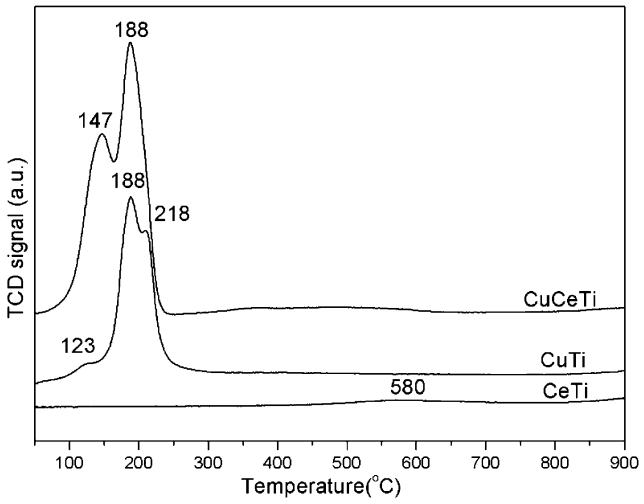

Figure 6. H_2-TPR profiles of the catalysts.

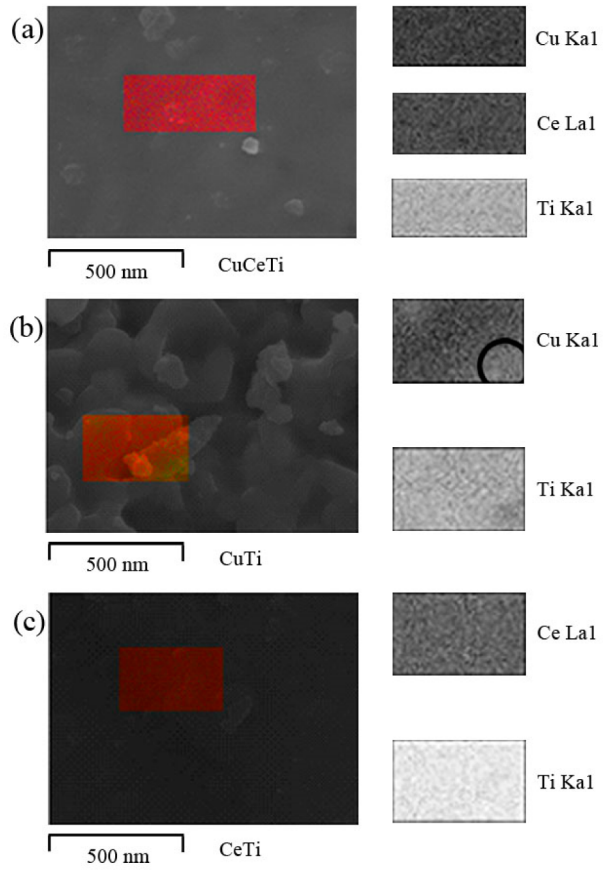

Figure 7. SEM images and EDS element mappings of (a) CuCeTi, (b) CuTi, and (c) CeTi catalysts.

the NH_3-SCR reaction is higher, implying enhancement by the presence of NO.

The ability of NO oxidation to NO_2 of the catalysts is shown in Figure 3. NO oxidation activity is higher on CuCeTi than CuTi below 300 °C; however, it becomes comparable at 300 °C and above. Contrastingly, the NO oxidation activity of the CeTi catalyst is quite low with only 7% NO oxidized to NO_2 at 350 °C. In general, results indicate copper-containing catalysts present significantly higher NO oxidation activity than CeTi. Zhang et al.[29] confirmed the increased generation of Lewis acid sites to be a plausible explanation for greater conversion of NO to NO_2 by Cu-supported mixed oxide samples.

The NO oxidation activity of the catalysts is crucial for the NH_3-SCR reaction, especially at temperatures below 250 °C. Centi et al.[30] verified that $Cu^{2+}-NO_2$ and $Cu^{2+}-N_2O_3$ species are important intermediates in NH_3-SCR reactions whereas Yang et al.[31] reported that an increase of NO oxidation to NO_2 on Fe-ZSM-5 catalysts leads to significant improvement in the SCR activity through the fast SCR route. Therefore, it is expected that high activity for NO to NO_2 conversion at low temperatures can also contribute to high SCR activity on CuCeTi catalysts.

3.2. XRD and BET. The XRD patterns of the catalysts are shown in Figure 4. Characteristic diffraction peaks of anatase TiO_2, rutile TiO_2 and CuO are detected from the CuTi catalyst with anatase, the dominate phase. The intense XRD peaks of CuO indicate a large presence of crystallized CuO. From the CeTi catalyst, only weak diffraction peaks of anatase are detected, indicating that strong interactions between ceria and TiO_2 lead to mutual dispersion of these two oxides. Similarly, the CuCeTi catalyst yields only very weak diffraction peaks of anatase TiO_2 and CuO, indicating that interactions among copper, ceria and anatase lead to high dispersions of these metal oxides. The copper species seems to be well-dispersed on CeO_x-TiO_2.[32] The composition, BET surface areas and particle size of the catalysts are listed in Table 1. Results indicate BET surface areas of the CuTi catalyst are much lower than that of the ceria-containing catalyst. Meanwhile, the BET surface areas of the CuCeTi catalyst are higher than those of the binary oxide catalysts and the average particle size of the CuCeTi catalyst is smaller than those of the binary oxide catalysts, which means the introduction of ceria lead to highly dispersed Cu species on catalyst surfaces.

3.3. UV–Vis Spectra. The UV–vis spectra of catalysts are shown in Figure 5. The results show that the spectra of CeTi and CuCeTi catalysts are dominated by the edge related to the O^{2-} to Ti^{4+} charge transfer of anatase below 400 nm.[33] The CeTi catalyst shows a strong absorption band at 380 nm due to the strong overlapping of charge transfers of anatase TiO_2 and CeO_2. The CuTi catalyst presents an absorption band at 337 nm, assigned to the charge transfer band of highly dispersed O–Cu–O complexes and a broad band at 600–800 nm, ascribed to the $d-d$ transitions of Cu^{2+} in bulk CuO.[34,35] The band at 600–800 nm of CuTi catalyst is much higher than that of the CuCeTi catalyst, which means there are more bulk Cu species on the CuTi catalyst, consistent with the XRD results. The broad band at 408 nm of CuCeTi can be assigned to the overlapped bands of charge transfers of anatase TiO_2, CeO_2 and O–Cu–O complexes, suggesting electronic interactions occur among CeO_2, CuO_x and anatase, which will facilitate the low temperature redox property of catalyst.

3.4. Redox Properties. The redox behaviors of the catalysts were characterized by H_2-TPR and the results are shown in Figure 6. For the CeTi catalyst, only a broad, weak peak centered at 580 °C is detected due to the stepwise reduction of Ce^{4+} to Ce^{3+} alongside strong interactions with TiO_2.[19,36] For the CuTi catalyst, a weak peak at 123 °C and a sharp peak at 188 °C with a shoulder at 218 °C were detected. A sharp bimodel peak at 147 and 188 °C was detected from the CuCeTi catalyst. Liu et al.[37,38] reported four types of copper sites: (a) isolated Cu^{2+} ions strongly interacting with the support; (b) weak magnetic associates consisting of several Cu^{2+} ions in close proximity; (c) small two- and three-

dx.doi.org/10.1021/am5004969 | ACS Appl. Mater. Interfaces 2014, 6, 8134–8145

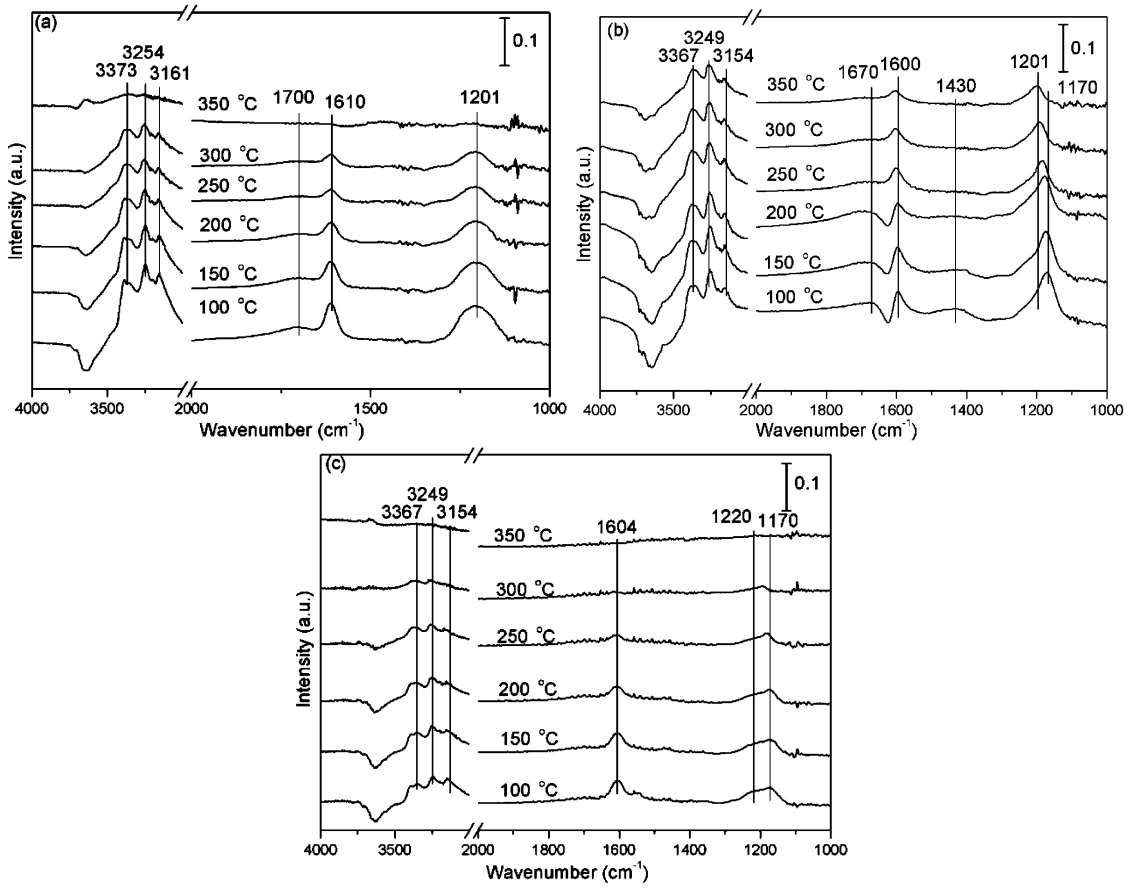

Figure 8. DRIFT spectra of adsorbed species on the (a) CuCeTi, (b) CeTi and (c) CuTi catalysts arising from contact with 1000 ppm of NH_3 balanced in N_2.

dimensional clusters with no specific or regular lattice arrangements; (d) large three-dimensional clusters and bulk phase CuO with characteristics and properties identical to those of pure CuO powder. Zhang et al.[29] reported that ceria introduction to a Cu/TiO_2 catalyst could increase the concentration of Cu^{2+}, yielding increased high mobility oxygen. Additionally, Shen et al.[39] confirmed that the high and stable redox properties of CeO_2 are significantly improved via formation of $Ce_{1-x}Cu_xO_y$ solid solutions.

With reference to the above summary, the reduction peaks at 123 and 147 °C may be attributed to reduction of isolated Cu^{2+} ions (a) or weak magnetic Cu^{2+} associates (b) with less interactions with the matrix, and those at 188 and 218 °C probably represent the reduction of CuO particles ($Cu^{2+} \rightarrow Cu^{+} \rightarrow Cu^{0}$) in small sizes with strong interactions with the CuCeTi matrix (c) and large bulk CuO particles with less interactions with the CuTi matrix (d). The H_2-TPR results indicate that the CuTi catalyst is mainly composed of two or three-dimensional clusters and bulk phase CuO. The introduction of ceria into the CuTi catalyst results in an increased reducibility of the CuO species as the peak maxima shifted to lower temperatures (218 to 188 °C and 188 to 147 °C, respectively) due to the enhanced dispersion of CuO arising from the improved interactions between CuO and the CeO_2-TiO_2 matrix.

3.5. SEM Images and Properties. The SEM images and EDS element mappings of CuCeTi catalysts are shown in Figure 7. The SEM images show that the CuCeTi and CeTi catalysts are more uniform than the CuTi catalyst. Meanwhile, the EDS element mappings show that Cu species are highly dispersed on the CuCeTi catalyst, whereas those on the CuTi catalyst are partly aggregated, as indicated by the circled zone in Figure 7b. The element mappings further confirm introduction of ceria improves the dispersion of Cu species, and decreases the particle sizes of catalysts simultaneously. Cerium species are both uniformly dispersed on CuCeTi and CeTi catalysts, indicating the strong structure interaction between ceria and anatase.

3.6. DRIFT Studies. *3.6.1. NH_3 Adsorption.* NH_3 adsorption on the catalysts was investigated by DRIFT, and the obtained spectra are shown in Figure 8. Strong bands at 1600−1610 and 1170−1220 cm^{-1} are observed for all the samples, respectively attributed to the σ_{as} and σ_s of NH_3 on Lewis acid sites.[40−43] The weak bands at 1700−1670 and 1430 cm^{-1} are respectively assigned to the σ_s and σ_{as} of NH_4^+ on Brønsted acid sites.[44] In the N−H region, several bands are observed at 3373, 3254 and 3161 cm^{-1}, corresponding to coordinated NH_3 on Lewis acid sites. A negative band at 3640 cm^{-1} is attributed to the O−H groups occupied by NH_3 adsorption.[45,46] The adsorption bands of the NH_3 species on the CuCeTi catalyst are much more intense than those on the CuTi catalyst, indicating increases in both Lewis and Brønsted acid sites from ceria addition.

As the temperature increases, all the bands of ammonia derived species decrease in intensity. Almost no bands are observed from adsorbed ammonia species on the surface of copper-containing catalysts at 350 °C, while they are still

dx.doi.org/10.1021/am5004969 | ACS Appl. Mater. Interfaces 2014, 6, 8134−8145

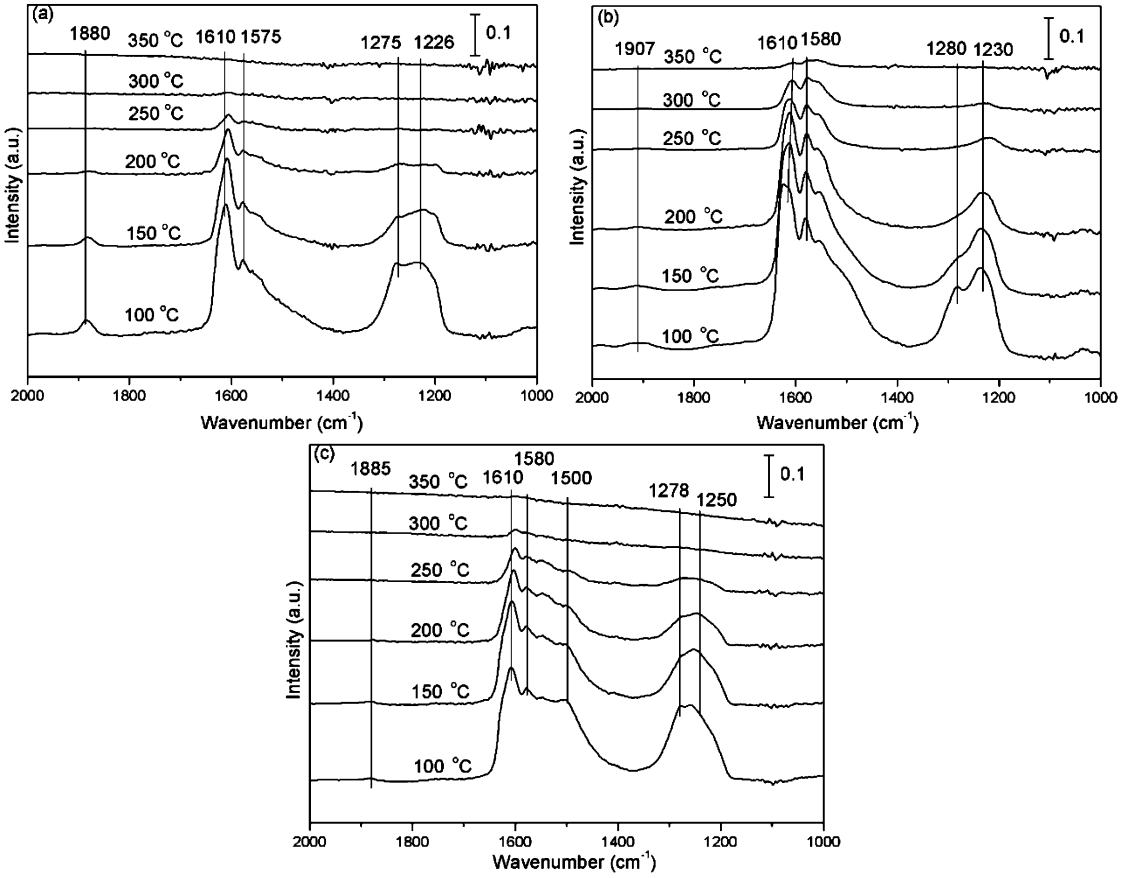

Figure 9. DRIFT spectra of adsorbed species on the (a) CuCeTi, (b) CeTi and (c) CuTi catalysts arising from contact with 1000 ppm of NO + 5% O_2, balanced in N_2.

prominent for the CeTi catalyst, indicating that the acidity of the CeTi catalyst is weakened by the copper oxides.

3.6.2. NO+O_2 Adsorption. The NO+O_2 adsorption of the catalysts was also investigated by DRIFT and the obtained spectra are shown in Figure 9. Bands at 1610, 1580−1575, 1280−1275 and 1226−1250 cm^{-1} were detected for all catalysts. The bands at 1580 and 1230 cm^{-1} were assigned to bidentate and bridged nitrate, whereas the bands at 1280 and 1610 cm^{-1} were attributed to monodentate nitrates, respectively.[47,48] Finally, the band at 1885 cm^{-1}, detected on the copper-containing catalysts, was assigned to weakly adsorbed copper mononitrosyls (Cu^{2+}−NO). It has been widely reported that Cu^{+} can be oxidized to Cu^{2+} in the presence of NO.[15,25] The band at 1885 cm^{-1} disappeared at 200 °C, indicating that the thermal stability of copper mononitrosyls is weak. The complex bands at 1500 cm^{-1} detected on the CuTi catalyst were also assigned to bidentate and monodentate nitrate.[49] The band at 1907 cm^{-1} on the CeTi catalyst can be assigned to weakly adsorbed NO.[41] It is clear that NO_x adsorbed on CeTi are much more stable than when adsorbed on copper-containing catalysts, suggesting that copper promotes the decomposition of nitrates on ceria catalysts.

3.6.3. Reaction between Nitrogen Oxides and Ammonia Adspecies. The DRIFT spectra of catalysts with preadsorbed NH_3 when exposed to NO+O_2 at 150 °C are shown in Figure 10. Generally, adsorbed NH_3 species decreased following NO_x introduction to the feed gas, indicating a reaction between NO_x and the adsorbed NH_3. Coordinated NH_3 (1170 cm^{-1}) and NH_4^{+} (1700 and 1670 cm^{-1}) species on the CeTi catalyst also disappeared quickly, accompanied by the appearance of new bands (1610 and 1245 cm^{-1}) corresponding to NO_x species after introduction of NO+O_2 for 2 min. However, the NO_x conversion of the CeTi catalyst at 150 °C was only around 5%, potentially due to the strong adsorption of NO_x rather than NH_3 onto active sites, which will be discussed later.

The NH_3-related bands on CuTi remain significant even after 10 min, although the bands for NO_x (1610, 1580, 1500 and 1278 cm^{-1}) are already significant. This result indicates that NH_3 and nitrite/nitrate can be adsorbed onto copper and titanium sites simultaneously. However, the NH_3-associated bands on the CuCeTi catalyst (N−H stretching region, 3373, 3254 and 3161 cm^{-1}) disappeared within 5 min and the nitrite/nitrate bands become dominant, which means that ceria accelerated the reaction between ad-NO_x and ad-NH_3.

3.6.4. Reaction between Ammonia and Nitrogen Oxides Adspecies. The DRIFT spectra of catalysts with preadsorbed NO+O_2 when exposed to NH_3 at 150 °C are shown in Figure 11. Unlike the preadsorbed NH_3, most of the preadsorbed NO_x species were relatively stable on catalysts even after the introduction of NH_3. Only one band at 1610 cm^{-1} ascribed to monodentate nitrate decreased simultaneously on all catalysts, indicating that some nitrates reacted with ammonia. The band annotated as bidentate nitrate (1580 cm^{-1}) vanished on the CuCeTi catalyst, while it was still significant on the CeTi and CuTi catalysts, indicating that preadsorbed NO_x on the binary oxide catalysts were quite stable and could not react with ammonia. Thus, the poor low-temperature NH_3-SCR activities

dx.doi.org/10.1021/am5004969 | ACS Appl. Mater. Interfaces 2014, 6, 8134−8145

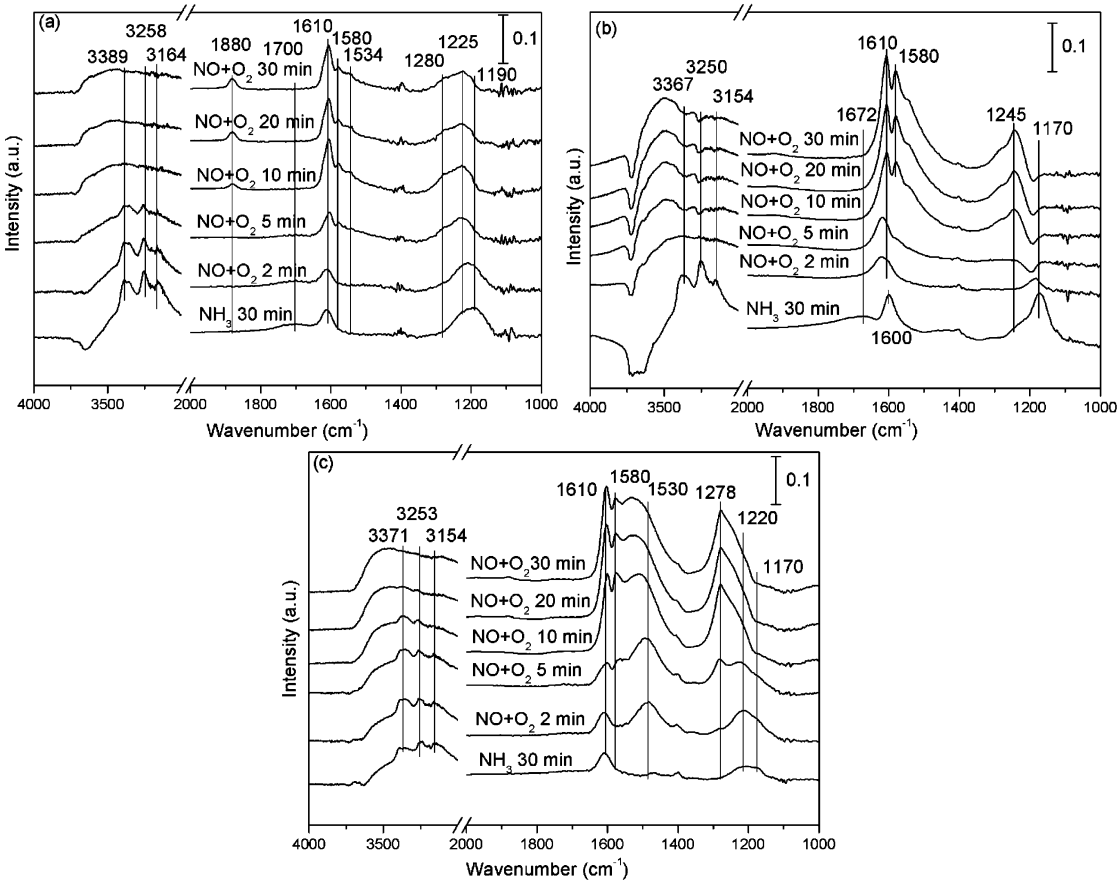

Figure 10. DRIFT spectra of adsorbed species on the (a) CuCeTi, (b) CeTi and (c) CuTi catalysts arising from contact with 1000 ppm of NO + 5% O_2 at 150 °C, N_2 balance. Pretreatment: 1000 ppm of NH_3 preadsorbed followed by N_2 purging for 30 min.

of CeTi and CuTi catalysts may be related to the inhibition of active sites by nitrates.

After purging with NH_3 for 5 min, new bands at 1700 and 1480−1490 cm^{-1} (NH_4^+ on Brønsted acid sites) and bands at 3393, 3253 and 3180 cm^{-1} (Lewis acid bonded NH_3) appeared for all catalysts. New bands assigned to NH_3 species appeared within 5 min with the remaining bands of NO_x species indicating NO_x and NH_3 could be coordinated to different sites.[47]

3.6.5. NH_3+NO+O_2 Coadsorption. The DRIFT spectra of catalysts following contact with NH_3+NO+O_2 at various temperatures are shown in Figure 12. In the N−H region, several bands assigned to coordinated NH_3 on Lewis acid sites (3373, 3254 and 3161 cm^{-1}) were detected in the spectra of all catalysts. Sharp, complex bands at 1610, 1580, 1280 and 1225 cm^{-1} were detected on the CuCeTi catalyst, most of which could be assigned to nitrate species overlapping with σ_{as} NH_3 on Lewis acid sites at 1600 cm^{-1}. The band at 1880 cm^{-1} was assigned to weakly adsorbed NO on the surface of the CuCeTi catalyst. Similar bands (1610, 1570, 1284 and 1225 cm^{-1}) with lower intensities were detected on the CuTi catalyst, except at 1480 cm^{-1}, which was related to the NO_2^-. These results indicate that most of the adsorbed NH_3 species react with NO_x species and strong NO_x bands remain on the surface of the CuCeTi and CuTi catalysts.

For the CeTi catalyst, Lewis acid site bonded NH_3 (1184 and 1600 cm^{-1}), Brønsted acid site bonded NH_4^+ (1470 and 1695 cm^{-1}) and nitrates (1560, 1508 and 1245 cm^{-1}) were all observed. The relatively stable adsorption of NH_3 species on both acid sites implies low SCR activity below 250 °C. The bands of coordinated NH_3 on Lewis acid sites decrease in intensity with increasing temperature and are completely absent above 250 °C, whereas those of the NH_4^+ on Brønsted acid sites persist even at high temperatures. Thus, NH_3 coordinated on Lewis acid sites is more active than NH_4^+ on the Brønsted acid sites at low temperatures, and the latter appears to be responsible for the high SCR activity of the CeTi catalyst at temperatures above 250 °C.

4. DISCUSSION

4.1. Catalytic Acidity. The role of acidic sites is important for NO_x reduction with NH_3. Activation and adsorption of NH_3 are considered to be key routes in the standard NH_3-SCR reaction. Busca et al.[40] reported that coordinated ammonia on Lewis acid sites was easily transformed by hydrogen abstraction to amide NH_2 species or to its dimeric form hydrazine N_2H_4, both of these species are intermediates in ammonia oxidation to N_2. Epling et al.[48] point out that an NH_4NO_3 intermediate was formed on Lewis acid sites on a Cu-SAPO-34 catalyst and the Brønsted acid sites acted as an NH_3 reservoir that supplied additional NH_3 for the SCR reaction via migration to Lewis acid sites. Kröcher et al.[49] reported that Lewis acid sites were the main active sites for NH_3 activation at low temperatures (<250 °C) and that Brønsted acid sites were not required for adsorption or activation of ammonia, however, were necessary to bind and disperse metal ions. Our previous work[15] confirmed that Lewis acid sites introduced by copper oxides assist formation of nitro compounds and rapid adsorption/

dx.doi.org/10.1021/am5004969 | ACS Appl. Mater. Interfaces 2014, 6, 8134−8145

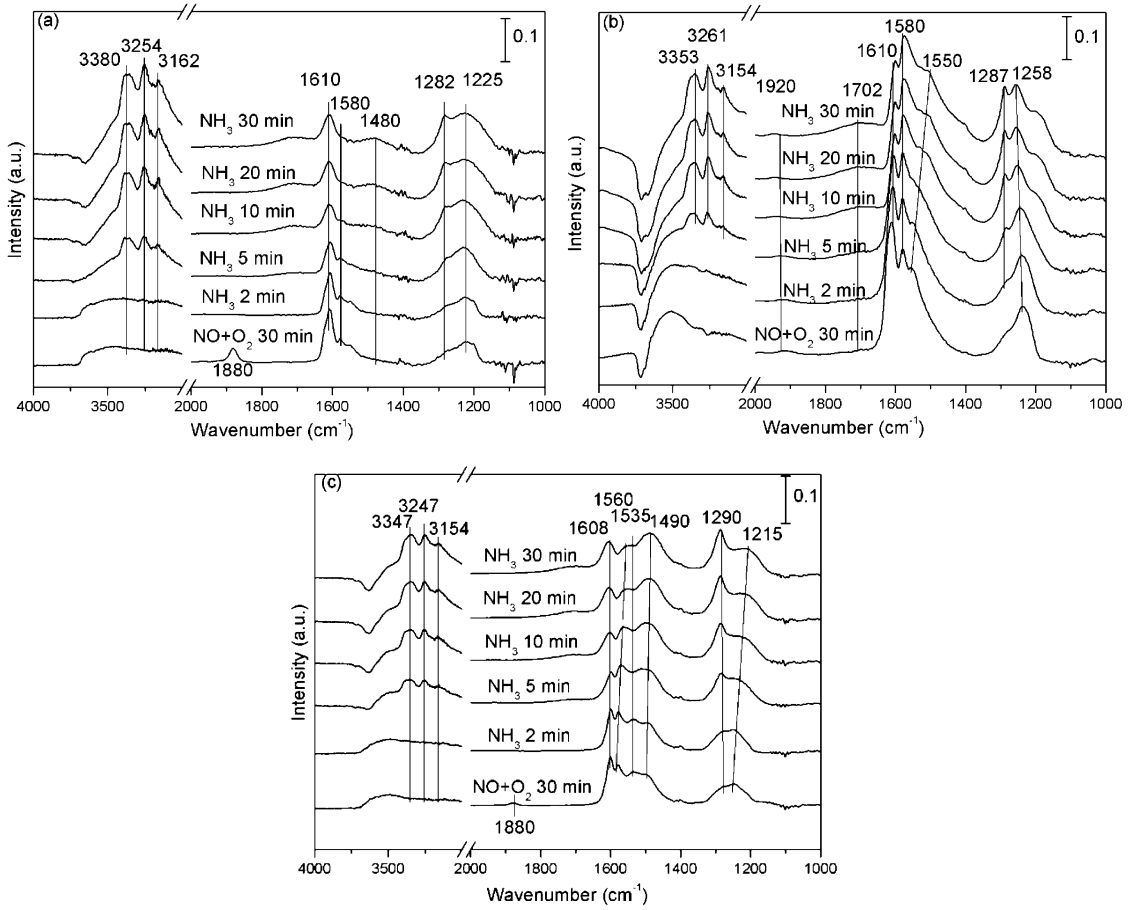

Figure 11. DRIFT spectra of adsorbed species on the (a) CuCeTi, (b) CeTi and (c) CuTi catalysts arising from contact with 1000 ppm of NH_3 + O_2 at 150 °C, N_2 balance. Pretreatment: 1000 ppm of NO + 5% O_2 preadsorbed followed by N_2 purging for 30 min.

desorption of NO/NO_2 onto catalysts, facilitating higher NH_3-SCR activity. Further work[50] confirmed that Lewis and Brønsted acid sites are the main adsorption sites for ammonia onto sulfated $NiO-CeO_2-ZrO_2$ catalysts.

In this work, the results of NH_3 adsorption (Figure 8) show that copper provides copious Lewis acid sites and cerium can provide both Lewis and Brønsted acid sites, both of which may strongly adsorb coordinated NH_3, NH_4^+, NH_2 and other intermediates from ammonia oxidations. According to the results of NH_3 and NO_x coadsorption (Figure 12), NH_3 species on Lewis and Brønsted acid sites persist on CeTi catalysts, while no distinct peak corresponding to NH_3 species on copper-containing catalysts is observable, indicating that most of the copper adsorbed NH_3 species reacted with NO_x species. On CuCeTi catalyst, ammonia activation predominantly occurs at Cu^{2+} Lewis acid sites. Furthermore, the introduction of ceria species generates increased Lewis and Brønsted acid sites, both of which can react with adsorbed NO_x at low temperatures, between 150 and 250 °C. Additionally, the introduction of ceria species also accelerates the reaction between NO_x and adsorbed NH_3, which confirms that Brønsted acid sites act as NH_3 reservoirs, supplying NH_3 for the SCR reaction via migration to the Lewis acid sites.

The results of DRIFT analyses suggest that ceria addition to CuTi catalysts increases both Lewis and Brønsted acidity. The enhanced Lewis acidity of CuCeTi catalyst may arise from greatly improved dispersion of copper oxides and titanium oxides by cerium oxides, which is supported by the XRD result and SEM images. Furthermore, oxygen vacancies form more easily in well-mixed metal oxides with different metal covalent bonds, as shown by H_2-TPR results. According to principles based on bond conservation order, a balance is expected between the strengths of $Ti^{n+}-O$ and O−H bonds in a $Ti^{n+}(OH)-O^*-Ce^{n+}$ unit, resulting in a correlation in which the shorter (stronger) $Ti^{n+}-O$ bond may yield to the longer $Ti^{n+}-O^*$ bond, and consequently weaken the O−H bond. A weak O−H bond results in the high ability of a $Ti^{n+}(OH)-O^*-Ce^{n+}$ center to release a proton to other molecules, hence enhancing Brønsted acidity.

The results of NH_3 adsorption for different catalysts are shown in Figure 13. From the results of the DRIFT studies, there is only a weak peak at 1480 cm^{-1}, assigned to the Brønsted acidity, which means the ammonia adsorption on CuCe is very weak and unstable. Therefore, it is reasonable that NH_3 is prone to stably adsorb onto titanium sites at low temperatures. Both Brønsted and Lewis acid sites are important for reduction of NO_x with NH_3. The adsorption and activation of ammonia are considered as the key steps in both standard NH_3-SCR and ammonia oxidation reactions. For CuCeTi catalysts, Cu^{n+} related Lewis acid sites are the main active sites for NH_3 and NO_x activation/oxidation. The H_2-TPR, NH_3/NO oxidation and NH_3/NO_x adsorption results indicate that the strong interactions among copper, cerium and titanium lead to highly dispersed metal oxides with high redox properties, which facilitate the ammonia activation/oxidation and NO oxidation at low temperatures.

dx.doi.org/10.1021/am5004969 | ACS Appl. Mater. Interfaces 2014, 6, 8134−8145

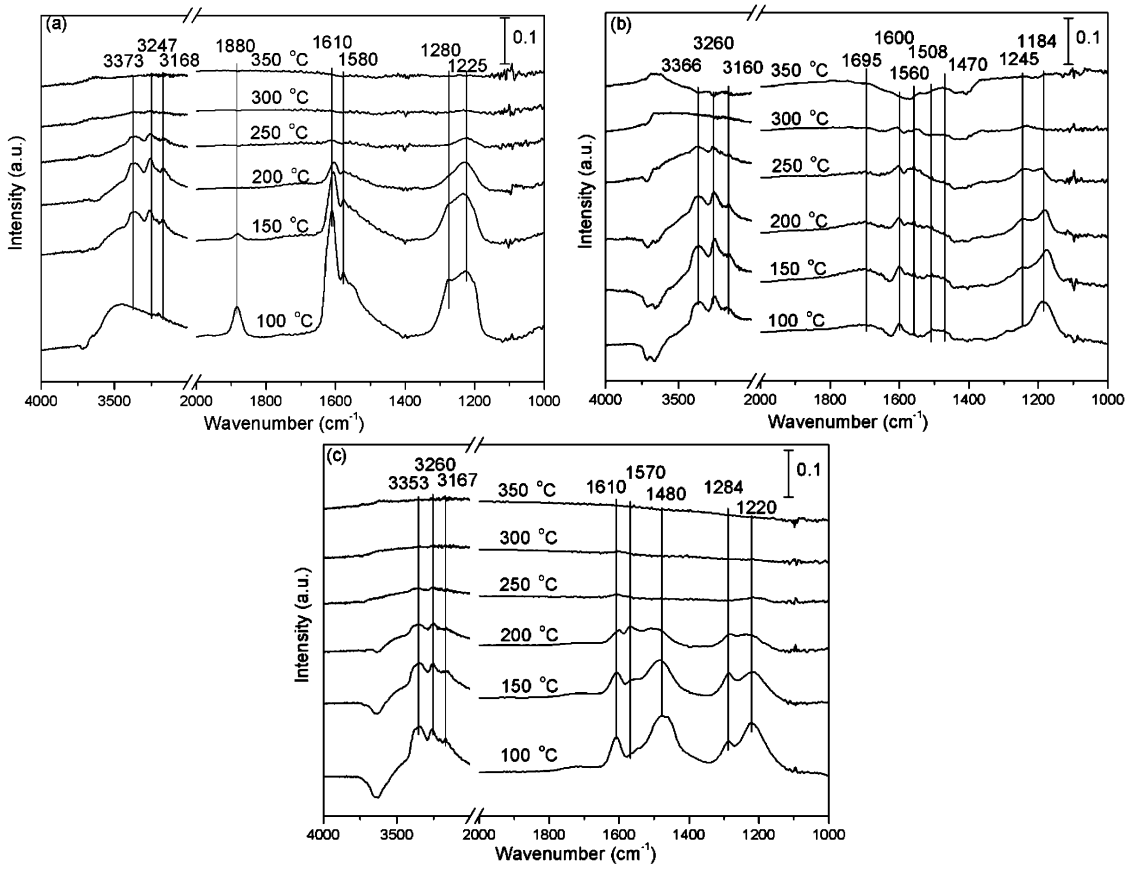

Figure 12. DRIFT spectra of adsorbed species arising from contact with 1000 ppm of NH_3 + 1000 ppm of NO + 5% O_2 at various temperatures over (a) CuCeTi, (b) CeTi and (c) CuTi catalysts.

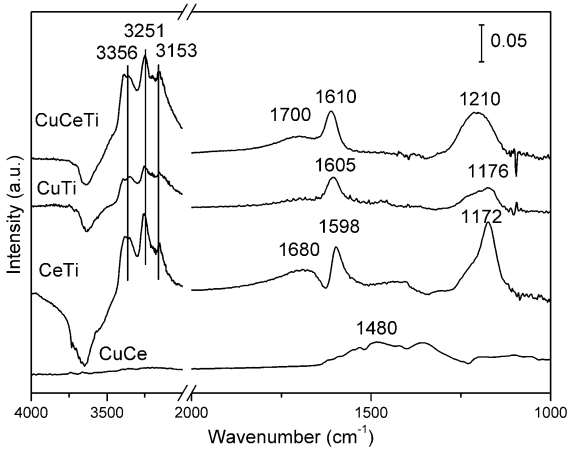

Figure 13. DRIFT spectra of adsorbed species on the CuCeTi catalysts arising from contact with 1000 ppm of NH_3 balanced in N_2 at 100 °C.

As temperature increases above 250 °C, the activity of Brønsted acid sites increases and the adsorption capability of Lewis acidity sites decreases, increasing the importance of Brønsted acid sites in the NH_3-SCR reaction. This is also the reason for high catalytic activity of the CeTi catalyst at temperatures above 250 °C.

4.2. NH_3-SCR Reaction Route on CuCeTi Catalyst at Low Temperatures. With respect to structure, the XRD, H_2-TPR and SEM image results indicate that introduction of ceria into a CuTi catalyst leads to high surface area and highly dispersed copper oxides on anatase TiO_2 support, predominantly in isolated or coupled Cu^{2+} ion forms. Simultaneously, increased oxygen adsorption, with high mobility, occurs due to the interaction between ceria and copper oxide. The Lewis acid sites from highly dispersed Cu^{2+} ions are the main active sites for NH_3 and NO_x activation/oxidation and are the main factor for higher NH_3-SCR activity ternary oxides catalysts in comparison to binary oxides catalysts.

Scheme 1. NH_3-SCR Reaction on CuCeTi Catalyst at Low Temperatures

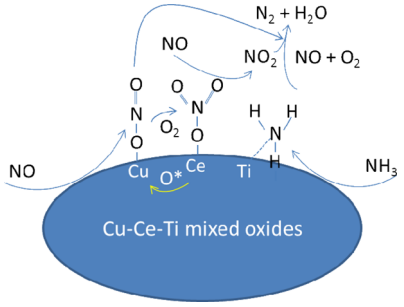

The mechanism of NH_3-SCR has been extensively studied in recent years, with both Langmuir–Hinshelwood (L–H) and Eley–Rideal (E–R) mechanisms proposed for different catalysts. Yang et al.[51] reported that the reaction pathway with a MnO_x–CeO_2 catalyst begins with the adsorption of NH_3 to form coordinated NH_3 and NH_2, followed by reactions with NO or HNO_2 to produce N_2 and H_2O. Li et al.[41] indicate that the NH_3-SCR mechanism with a CeWTi catalyst might mainly

dx.doi.org/10.1021/am5004969 | ACS Appl. Mater. Interfaces 2014, 6, 8134–8145

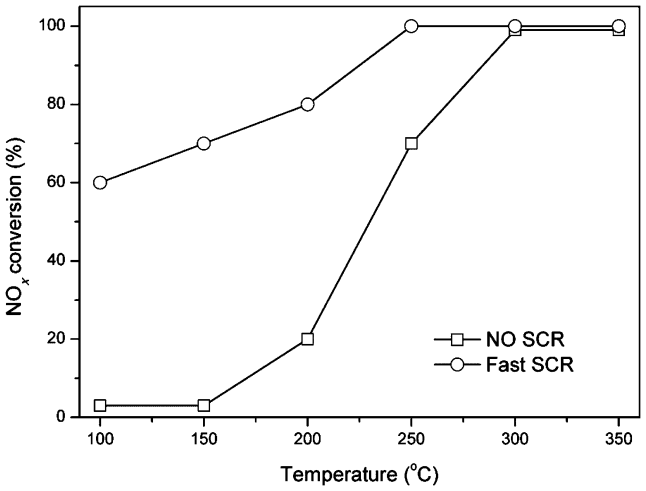

Figure 14. Fast SCR behavior of CeTi catalyst. Reaction conditions: $[NH_3]$ = 500 ppm, $[NO]$ = $[NO_2]$ = 250 ppm, $[O_2]$ = 5%, balanced in N_2, GHSV = 30 000 h^{-1}.

follow an E−R mechanism including NH_3 adsorption and intermediate NH_2 reacting with gaseous NO to form N_2 and H_2O. Tronconi et al.[7] investigated the NO/NO_2−NH_3 SCR reaction over a commercial Fe-ZSM-5 catalyst, showing that fast SCR started with NO_2 dimerization to form nitrates and nitrites, which react with adsorbed NH_3 species to form NH_4NO_3 and NH_4NO_2. NH_4NO_2 rapidly decomposes to N_2 and H_2O and the reduction of NH_4NO_3 by NO is the limiting step, which is inhibited by NH_3. A similar reaction pathway was also proposed for the NH_3-SCR reaction over the Cu-SAPO-34 catalyst.[48]

From the results of the DRIFT studies on the CuCeTi catalyst, all evidence indicated that highly dispersed, isolated or coupled Cu^{2+} ions are the main active sites for NH_3 and NO_x activation/oxidation. When $NO+O_2$ passes over preadsorbed NH_3 on the CuCeTi catalyst, all of the NH_3 related bands quickly disappeared, while NH_3 passing over preadsorbed the $NO+O_2$ only removed certain nitrates (monodentate and bidentate), which were replaced by NH_3 associated bands. These results indicate that both adsorbed NH_3 and NO_x could participate in the NH_3-SCR reaction over a ternary oxide catalyst. In the NH_3+NO+O_2 coadsorption experiment, Cu^{2+}−NO, nitrates and NH_3 derived species were all observed simultaneously on the CuCeTi catalyst at 150 °C, indicating these species are important intermediates in NH_3-SCR reactions. A large amount of nitrates can stably adsorb on ceria sites and copper species facilitate the decomposition of nitrates. NO may react with NH_4NO_3 to generate $N_2+H_2O+NO_2$ (eq 4).[45,52] The generated NO_2 can participate in the fast SCR reaction on the surface of the CuCeTi catalyst. Well-dispersed copper oxide and ceria on titanium may promote the reaction between NH_3, NO and NH_4NO_3 via shortening the distance between these reactants.

$$NH_4NO_3 + NO \rightarrow N_2 + 2H_2O + NO_2 \quad (4)$$

In this work, increased redox properties of CuCeTi catalysts also led to the formation of N_2O, which is one of the major drawbacks for low-temperature NH_3-SCR, as it decreases the N_2 selectivity and the deNO_x efficiency. Research carried out by Suárez et al.[53] proposed that ammonia oxidation was not the main path for the N_2O formation, instead suggesting the reaction between $NO_3^-{}_{(ads)}$ and $NH_{x(ads)}$ species adsorbed on Cu^{2+} to be the feasible path. Grossale et al.[54] and Iwasaki et al.[9] pointed out that in the fast SCR reaction, N_2O comes from thermal decomposition of ammonium nitrate, and the highest N_2O selectivities are detected in response to high NO_2 addition to NO_x feed contents. On copper-containing catalysts, formation of N_2O starts at 150 °C and peaks at 300 °C during the SCR reaction, whereas the onset temperature of N_2O formation is 200 °C in NH_3 oxidation. The amount of N_2O generated during the NH_3-SCR reaction is much larger than that generated from NH_3 oxidation. These results suggest that the majority of N_2O formation is not only due to NH_3 oxidation but also to thermal decomposition of NH_4NO_3 (eq 5) at low temperatures. However, the similar N_2O generation profile of NH_3-SCR and NH_3 oxidation, and the significant generation of N_2O in NH_3 oxidation, strongly suggest that ammonia oxidation also plays a partial role in N_2O generation at high temperatures (>200 °C).

$$NH_4NO_3 \rightarrow N_2O + 2H_2O \quad (5)$$

The main NH_3-SCR reaction route at low temperatures on a CuCeTi catalyst is shown in Scheme 1. Simplistically, active oxygen arising from strong interactions among metal oxides is important to oxidize the Cu^{2+}−NO species into nitrates, which will be stored on cerium sites or directly participate in the fast SCR reaction. Alternatively, NH_3 preferentially adsorbs on titanium sites and then participates in both "standard SCR" and fast SCR reactions at low temperatures (<250 °C). The activity comparison of CeTi in standard SCR and fast SCR reactions is shown Figure 14. It is clear that NO_2 in the reactant promotes NO_x conversion on CeTi catalysts at low temperatures. Both low-temperature catalytic activity and N_2 selectivity is better than that of ternary-component catalysts. This result strengthens the assertion that both NH_3 activation and NO_2 formation lead to the increased low-temperature activity of ternary component catalysts but that the fast SCR reaction is dominant on catalysts at low temperatures.

5. CONCLUSIONS

A $CuO-CeO_2-TiO_2$ catalyst synthesized by a sol−gel method presents high NH_3-SCR activity (>80%) in a low temperature range of 150−250 °C. The strong structural interactions between copper, cerium and titanium oxides lead to highly dispersed metal oxides and adsorbed oxygen with high mobility, which improves the redox properties of the $CuO-CeO_2-TiO_2$ ternary oxide catalyst, leading to the excellent low-temperature activity of the catalyst. Lewis acid sites generated from highly dispersed Cu^{2+} ions are the main active sites for NH_3 and NO_x activation/oxidation and NH_3 preferentially adsorbs on titanium sites. Thus, the NH_3-SCR reaction routes over the $CuO-CeO_2-TiO_2$ ternary oxide are proposed to mainly happen between Cu^{2+}−NO, nitrate coordinated on cerium sites and titanium sites bonded with ammonia. The active oxygen arising from the strong interactions among metal oxides is important to oxidize the Cu^{2+}−NO species to nitrates, which will be stored on cerium sites or directly participate in the fast SCR reaction.

AUTHOR INFORMATION

Corresponding Author

*Duan Weng, Professor. E-mail: duanweng@mail.tsinghua.edu.cn.

Author Contributions

The paper was written through contributions of all authors. All authors have given approval to the final version of the paper.

Notes

The authors declare no competing financial interest.

■ ACKNOWLEDGMENTS

We acknowledge the Ministry of Science and Technology, PR China for financial support of Projects 2010CB732304 and 2013AA065302 and National Natural Science Foundation of China for the financial support of Project 51202126 and 51372137.

■ REFERENCES

(1) Busca, G.; Liette, L.; Ramis, G.; Berti, F. Chemical and Mechanistic Aspects of the Selective Catalytic Reduction of NO_x by Ammonia over Oxide Catalysts: A Review. *Appl. Catal., B* **1998**, *18*, 1−36.

(2) Li, J. H.; Chang, H.; Ma, Z.; Hao, L.; M, J.; Yang, R. T. Low-temperature Selective Catalytic Reduction of NO_x with NH_3 over Metal Oxide and Zeolite Catalysts—A Review. *Catal. Today* **2011**, *175*, 147−156.

(3) Irfan, M. F.; Goo, J. H.; Kim, S. D. Co_3O_4 based Catalysts for NO Oxidation and NO_x Reduction in Fast SCR Process. *Appl. Catal., B* **2008**, *78*, 267−274.

(4) Xu, W. Q.; Yu, Y. B.; Zhang, C. B.; He, H. Selective Catalytic Reduction of NO by NH_3 over a Ce/TiO_2 Catalyst. *Catal. Commun.* **2008**, *9*, 1453−1457.

(5) Kato, A.; Matsuda, S.; Kamo, T.; Nakajima, F.; Kuroda, H.; Narita, T. *J.* Reaction between NO_x and NH_3 on Iron Oxide-Titanium Oxide Catalyst. *Phys. Chem.* **1981**, *85*, 4099−4102.

(6) Koebel, M.; Madia, G.; Elsener, M. Selective Catalytic Reduction of NO and NO_2 at Low Temperatures. *Catal. Today* **2002**, *73*, 239−247.

(7) Grossale, A.; Nova, I.; Tronconi, E.; Chatterjee, D.; Weibel, M. The Chemistry of the $NO/NO_2−NH_3$ "fast" SCR Reaction over Fe-ZSM5 Investigated by Transient Reaction Analysis. *J. Catal.* **2008**, *256*, 312−322.

(8) Tronconi, E.; Nova, I.; Ciardelli, C.; Chatterjee, D.; Weibel, M. Redox Features in the Catalytic Mechanism of the "Standard" and "Fast" NH_3-SCR of NO_x over a V-based Catalyst Investigated by Dynamic Methods. *J. Catal.* **2007**, *245*, 1−10.

(9) Iwasaki, M.; Shinjoh, H. A Comparative Study of "Standard", "Fast" and "NO_2" SCR Reactions over Fe/zeolite Catalyst. *Appl. Catal., A* **2010**, *390*, 71−77.

(10) Nova, I.; Ciardelli, C.; Tronconi, E.; Chatterjee, D.; Bandl-Konrad, B. $NH_3−NO/NO_2$ Chemistry over V-based Catalysts and its Role in the Mechanism of the Fast SCR Reaction. *Catal. Today* **2006**, *114*, 3−12.

(11) Ruggeri, M. P.; Grossale, A.; Nova, I.; Tronconi, E.; Jirglova, H.; Sobalik, Z. FTIR in situ Mechanistic Study of the NH_3 NO/NO_2 "Fast SCR" Reaction over a Commercial Fe-ZSM-5 Catalyst. *Catal. Today* **2012**, *184*, 107−114.

(12) Stanciulescu, M.; Caravaggio, G.; Dobri, A.; Moir, J.; Burich, R.; Charland, J. P.; Bulsink, P. Low-temperature Selective Catalytic Reduction of NO_x with NH_3 over Mn-containing Catalysts. *Appl. Catal., B* **2012**, *123−124*, 229−240.

(13) Si, Z. C.; Weng, D.; Wu, X. D.; Jiang, Y.; Wang, B. Modifications of $CeO_2−ZrO_2$ Solid Solutions by Nickel and Sulfate as Catalysts for NO Reduction with Ammonia in Excess O_2. *Catal. Commun.* **2010**, *11*, 1045−1048.

(14) Zhou, C. C.; Zhang, Y. P.; Wang, X. L.; Xu, H. T.; Sun, K. Q.; Shen, K. Influence of the Addition of Transition Metals (Cr, Zr, Mo) on the Properties of $MnO_x−FeO_x$ Catalysts for Low-temperature Selective Catalytic Reduction of NO_x by Ammonia. *J. Colloid Interface Sci.* **2013**, *392*, 319−324.

(15) Si, Z. C.; Weng, D.; Wu, X. D.; Li, J.; Li, G. Structure, Acidity and Activity of CuO_x/WO_x-ZrO_2 Catalyst for Selective Catalytic Reduction of NO by NH_3. *J. Catal.* **2010**, *271*, 43−51.

(16) Sullivan, J. A.; Doherty, J. A. NH_3 and Urea in the Selective Catalytic Reduction of NO_x over Oxide-supported Copper Catalysts. *Appl. Catal., B* **2005**, *55*, 185−194.

(17) Zhou, J.; Gao, F.; Dong, L. H.; Yu, W. Y.; Qi, L.; Wang, Z.; Dong, L.; Chen, Y. Studies on Surface Structure of $M_xO_y/MoO_3/CeO_2$ System (M = Ni, Cu, Fe) and its Influence on SCR of NO by NH_3. *Appl. Catal., B* **2010**, *95*, 144−152.

(18) Thirupathi, B.; Smirniotis, P. G. Co-doping a Metal (Cr, Fe, Co, Ni, Cu, Zn, Ce, and Zr) on Mn/TiO_2 Catalyst and its Effect on the Selective Reduction of NO with NH_3 at Low-temperatures. *Appl. Catal., B* **2011**, *110*, 195−206.

(19) Gao, X.; Jiang, Y.; Fu, Y. C.; Zhong, Y.; Luo, Z. Y.; Cen, K. F. Preparation and Characterization of CeO_2/TiO_2 Catalysts for Selective Catalytic Reduction of NO with NH_3. *Catal. Commun.* **2010**, *11*, 465−469.

(20) Ito, E.; Mergler, Y. J.; Nieuwenhuys, B. E.; van Bekkum, H.; van den Bleek, C. M. Infrared Studies of NO Adsorption and Co-adsorption of NO and O_2 onto Cerium-exchanged Mordenite (CeNaMOR). *Microporous Mater.* **1995**, *4*, 455−465.

(21) Gu, T. T.; Liu, Y.; Weng, X. L.; Wang, H. Q.; Wu, Z. B. The Enhanced Performance of Ceria with Surface Sulfation for Selective Catalytic Reduction of NO by NH_3. *Catal. Commun.* **2010**, *12*, 310−313.

(22) Li, P.; Xin, Y.; Li, Q.; Wang, Z. P.; Zhang, Z. L.; Zheng, L. R. Ce−Ti Amorphous Oxides for Selective Catalytic Reduction of NO with NH_3: Confirmation of Ce−O−Ti Active Sites. *Environ. Sci. Technol.* **2012**, *46*, 9600−9605.

(23) Shan, W. P.; Liu, F. D.; He, H.; Shi, X. Y.; Zhang, C. B. An Environmentally-benign CeO_2-TiO_2 Catalyst for the Selective Catalytic Reduction of NO_x with NH_3 in Simulated Diesel Exhaust. *Catal. Today* **2012**, *184*, 160−165.

(24) Shan, W. P.; Liu, F. D.; He, H.; Shi, X. Y.; Zhang, C. B. A Superior Ce-W-Ti Mixed Oxide Catalyst for the Selective Catalytic Reduction of NO_x with NH_3. *Appl. Catal., B* **2012**, *115−116*, 100−106.

(25) Gao, X.; Du, X. S.; Cui, L. W.; Fu, Y. C.; Luo, Z. Y.; Cen, K. F. A Ce-Cu-Ti Oxide Catalyst for the Selective Catalytic Reduction of NO with NH_3. *Catal. Commun.* **2010**, *12*, 255−258.

(26) Du, X. S.; Gao, X.; Cui, L. W.; Fu, Y. C.; Luo, Z. Y.; Cen, K. F. Investigation of the Effect of Cu Addition on the SO_2-resistance of a Ce-Ti Oxide Catalyst for Selective Catalytic Reduction of NO with NH_3. *Fuel* **2012**, *92*, 49−55.

(27) Du, X. S.; Gao, X.; Cui, L. W.; Zheng, Z. Z.; Ji, P. D.; Luo, Z. Y.; Cen, K. F. Experimental and Theoretical Studies on the Influence of Water Vapor on the Performance of a Ce-Cu-Ti Oxide SCR Catalyst. *Appl. Surf. Sci.* **2013**, *270*, 370−376.

(28) Suárez, S.; Jung, S. M.; Avila, P.; Grange, P. Blanco, Influence of NH_3 and NO Oxidation on the SCR Reaction Mechanism on Copper/nickel and Vanadium Oxide Catalysts Supported on Alumina and Titania. *Catal. Today* **2002**, *75*, 331−338.

(29) Liu, J.; Li, X. Y.; Zhao, Q. D.; Zhang, D. K.; Ndokoye, P. The Selective Catalytic Reduction of NO with Propene over Cu-supported Ti−Ce Mixed Oxide Catalysts: Promotional Effect of Ceria. *J. Mol. Catal. A: Chem.* **2013**, *378*, 115−123.

(30) Centi, G.; Perathoner, S.; Biglino, D.; Giamello, E. Adsorption and Reactivity of NO on Copper-on-Alumina Catalysts: I. Formation of Nitrate Species and Their Influence on Reactivity in NO and NH_3 Conversion. *J. Catal.* **1995**, *152*, 75−92.

(31) Long, R. Q.; Yang, R. T. Catalytic Performance of Fe-ZSM-5 Catalysts for Selective Catalytic Reduction of Nitric Oxide by Ammonia. *J. Catal.* **1999**, *188*, 332−339.

(32) Zhu, H. Y.; Shen, M. M.; Kong, Y.; Hong, J. M.; Hu, Y. H.; Liu, T. D.; Dong, L.; Chen, Y.; Jian, C.; Liu, Z. Characterization of Copper Oxide Supported on Ceria-modified Anatase. *J. Mol. Catal. A: Chem.* **2004**, *219*, 155−164.

(33) Larrubia, M. A.; Busca, G. An Ultraviolet−Visible−Near Infrared Study of the Electronic Structure of Oxide-supported Vanadia−Tungsta and Vanadia−Molybdena. *Mater. Chem. Phys.* **2001**, *72*, 337−346.
(34) Kecht, J.; Tahri, Z.; Waele, D.; Mostafavi, M.; Mintova, S.; Bein, T. Colloidal Zeolites as Host Matrix for Copper Nanoclusters. *Chem. Mater.* **2006**, *18*, 3373−3380.
(35) Gu, J. L.; Huang, Y.; Elangovan, S. P.; Li, Y. S.; Zhao, W. R.; Toshio, L.; Yamazaki, Y.; Shi, J. L. Highly Dispersed Copper Species within SBA-15 Introduced by the Hydrophobic Core of a Surfactant Micelle as a Carrier and Their Enhanced Catalytic Activity for Cyclohexane Oxidation. *J. Phys. Chem. C* **2011**, *115*, 21211−21217.
(36) Wu, Z. W.; Zhu, H. Q.; Qin, Z. F.; Wang, H.; Huang, L. C.; Wang, J. G. Preferential Oxidation of CO in H_2-rich Stream over $CuO/Ce_{1-x}Ti_xO_2$ Catalysts. *Appl. Catal., B* **2010**, *98*, 204−212.
(37) Liu, Z. G.; Zhou, R. X.; Zheng, X. M. Comparative Study of Different Methods of Preparing $CuO-CeO_2$ Catalysts for Preferential Oxidation of CO in Excess Hydrogen. *J. Mol. Catal. A: Chem.* **2007**, *267*, 137−142.
(38) Liu, Z. G.; Zhou, R. X.; Zheng, X. M. Preferential Oxidation of CO in Excess Hydrogen over a Nanostructured $CuO−CeO_2$ Catalyst with High Surface Areas. *Catal. Commun.* **2008**, *9*, 2183−2186.
(39) Shan, W. J.; Shen, W. J.; Li, C. Structural Characteristics and Redox Behaviors of $Ce_{1-x}Cu_xO_y$ Solid Solutions. *Chem. Mater.* **2003**, *15*, 4761−4767.
(40) Ramis, G.; Yi, L.; Busca, G.; Turco, M.; Kurco, E.; Willey, R. J. Adsorption, Activation, and Oxidation of Ammonia over SCR Catalysts. *J. Catal.* **1995**, *157*, 523−535.
(41) Chen, L.; Li, J. H.; Ge, M. F. DRIFT Study on Cerium−Tungsten/Titiania Catalyst for Selective Catalytic Reduction of NO_x with NH_3. *Environ. Sci. Technol.* **2010**, *44*, 9590−9596.
(42) Larrubia, M. A.; Ramis, G.; Busca, G. An FT-IR Study of the Adsorption and Oxidation of N-containing Compounds over Fe_2O_3-TiO_2 SCR Catalysts. *Appl. Catal., B* **2001**, *30*, 101−110.
(43) Larrubia, M. A.; Ramis, G.; Busca, G. An FT-IR Study of the Adsorption of Urea and Ammonia over $V_2O_5−MoO_3−TiO_2$ SCR catalysts. *Appl. Catal., B* **2000**, *27*, L145−L151.
(44) Zawadzki, J.; Wisniewski, M. In situ Characterization of Interaction of Ammonia with Carbon Surface in Oxygen Atmosphere. *Carbon* **2003**, *41*, 2257−2267.
(45) Sun, D. K.; Liu, Q. Y.; Liu, Z. Y.; Gui, G. Q.; Huang, Z. G. Adsorption and Oxidation of NH_3 over V_2O_5/AC Surface. *Appl. Catal., B* **2009**, *92*, 462−467.
(46) Ramis, G.; Yi, L.; Busca, G. Ammonia Activation over Catalysts for the Selective Catalytic Reduction of NO_x and the Selective Catalytic Oxidation of NH_3. An FT-IR Study. *Catal. Today* **1996**, *28*, 373−380.
(47) Chen, L.; Li, J. H.; Ge, M. F. Promotional Effect of Ce-doped V_2O_5-WO_3/TiO_2 with Low Vanadium Loadings for Selective Catalytic Reduction of NO_x by NH_3. *J. Phys. Chem. C* **2009**, *113*, 21177−21184.
(48) Wang, D.; Zhang, L.; Kamasamudram, K.; Epling, W. S. In Situ-DRIFTS Study of Selective Catalytic Reduction of NO_x by NH_3 over Cu-Exchanged SAPO-34. *ACS Catal.* **2013**, *3*, 871−881.
(49) Brandenberger, S.; Kröcher, O.; Wokaun, A.; Tissler, A.; Althoff, R. The Role of Brønsted Acidity in the Selective Catalytic Reduction of NO with Ammonia over Fe-ZSM-5. *J. Catal.* **2009**, *268*, 297−306.
(50) Si, Z. C.; Weng, D.; Wu, X. D.; Ma, Z. R.; Ma, J.; Ran, R. Lattice Oxygen Mobility and Acidity Improvements of $NiO−CeO_2−ZrO_2$ Catalyst by Sulfation for NO_x Reduction by Ammonia. *Catal. Today* **2013**, *201*, 122−130.
(51) Qi, G.; Yang, R. T.; Chang, R. MnO_x-CeO_2 Mixed Oxides Prepared by Co-Precipitation for Selective Catalytic Reduction of NO with NH_3 at Low Temperatures. *Appl. Catal., B* **2004**, *51*, 93−106.
(52) Hadjiivanov, K. I. Identification of Neutral and Charged N_xO_y Surface Species by IR Spectroscopy. *Catal. Rev. Sci. Eng.* **2000**, *42*, 71−144.
(53) Suárez, S.; Martín, J. A.; Yates, M.; Avila, P.; Blanco, J. N_2O Formation in the Selective Catalytic Reduction of NO_x with NH_3 at Low Temperature on CuO-Supported Monolithic Catalysts. *J. Catal.* **2005**, *229*, 227−236.
(54) Grossale, A.; Nova, I.; Troncoi, E. Study of a Fe−Zeolite-Based System as NH_3-SCR Catalyst for Diesel Exhaust Aftertreatment. *Catal. Today* **2008**, *136*, 18−27.